Neutron-induced transmutations, gas production, and helium embrittlement of fusion materials.

M.R. Gilbert*, S.L. Dudarev, S. Zheng, L.W. Packer, J.-Ch. Sublet

EURATOM/CCFE Fusion Association, Culham Centre for Fusion Energy, Abingdon, Oxfordshire OX14 3DB, UK.

Abstract

In a fusion reactor, materials will be subjected to significant fluxes of high-energy neutrons. As well as causing radiation damage, the neutrons also initiate nuclear reactions leading to changes in the chemical composition of materials (transmutation). Many of these reactions produce gases, particularly helium, which cause additional swelling and embrittlement of materials. This paper investigates, using both neutronics and inventory calculations, the variation in gas production levels (and transmutation rates) as a function of position within the high flux regions of a recent conceptual model for the 'next-step' fusion device DEMO. Additionally, simple modelling of grain structures and gas diffusion rates illustrates that the lifetime of components, limited by He embrittlement, varies widely between different materials.

1. Introduction

In both planned and future fusion devices one of the key outstanding issues for researchers lies in the understanding of how materials are affected by the high fluxes of neutrons produced by the fusion plasmas. Not only do the incident neutrons cause atomic displacements within materials surrounding the plasma, leading to defect accumulation, but they can also initiate non-elastic nuclear reactions that cause the atoms of a material to be altered (transmuted), leading to a change in the structure and behaviour of components. Even more problematic, are the subset of the possible nuclear reactions that produce gas particles (helium and hydrogen). Helium in particular, with its low reactivity, can persist in materials over long periods of time, leading to accumulation in existing cracks or at grain boundaries, which can then result in swelling or embrittlement.

Since many of these gas-producing nuclear reactions have thresholds, gas production and any subsequent swelling is more of a concern in fusion compared to fission because of the larger fraction of neutrons at higher energies and higher overall flux (see for example, figure 1, which compares the neutron flux per lethargy interval[1] as a function of energy for the 3.0 GWt [gigawatts of thermal power] DEMO concept to a 3.8 GWt fission reactor).

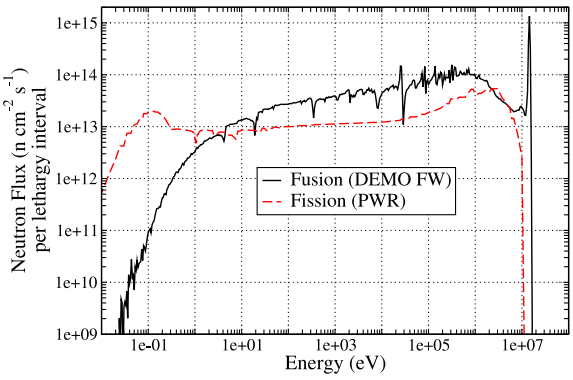

Figure 1: Comparison of the neutron-energy spectra in fission and fusion reactors. Shown is the average neutron spectrum in the fuel-assembly of a PWR reactor and the equatorial FW spectrum for the DEMO model in figure 2.

This paper describes the latest results from neutron-induced transmutation calculations as a

*Corresponding author email: mark.gilbert@ccfe.ac.uk

[1] a lethargy interval is the standard measure for spectra of this type, and is equal to the natural logarithm of the ratio of a given energy-interval's upper bound to its lower bound.

function of position in a conceptual design of DEMO – the demonstration fusion power-plant. We also develop a simple model for the accumulation of He at grain boundaries and, using results from the neutronics and inventory calculations, estimate the timescales associated with embrittlement of different materials in a fusion environment.

2. Neutron-induced transmutation of materials

Previous works [1] have focused on the transmutation response of various materials under identical first wall (FW) conditions. Here we go further to investigate the response of materials as a function of position within a fusion device, with particular emphasis on how gas production rates change.

2.1. Geometry dependence of neutron flux and energy spectrum

Neutron spectra have been calculated for different regions of a recent DEMO design, proposed by CCFE in 2009 [2], (see figure 2) using the neutron-transport code MCNP [3]. The model is highly simplified, with only the major structures included, and with homogeneous material compositions. Several of the spectra calculated for this model are shown in figure 3.

Both the energy profile and fluxes of the neutron spectra vary dramatically as a function of depth into the equatorial region of the FW at A in figure 2. Not only does the spectrum of energies become heavily moderated as the depth increases, but the flux also falls greatly – from 8.25×10^{14} n cm^{-2} s^{-1} in the 2 cm FW at position A, to 3.9×10^{13} n cm^{-2} s^{-1} in the final five cm of the blanket.

Within the divertor the neutron flux and spectrum also show significant variation as a function of position (see figure 3b). At point E in figure 2, the total flux in the 2 cm layer of pure W divertor armour, is approximately twice as high as that at G (7.1×10^{14} n cm^{-2} s^{-1} at E compared to 3.6×10^{14} n cm^{-2} s^{-1} at G).

2.2. Influence on transmutation and gas production

The calculated neutron spectra and total fluxes for the DEMO model have been used in the inventory code FISPACT [4] to simulate the burn-up (transmutation) of various materials relevant to design. FISPACT requires an external library of reaction cross sections and decay data, and here we have

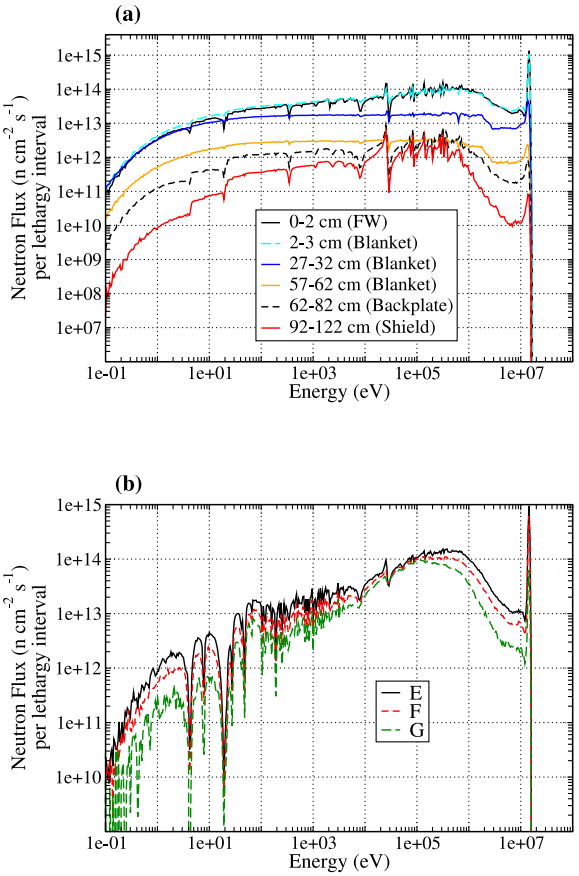

Figure 3: Comparison of the neutron-energy spectra in DEMO; (a) as a function of depth into different regions of the containment vessel at the equatorial position (A) in figure 2; and (b) in the divertor-armour layer as a function of position ((E–G) in 2)

employed the 2003 version of the European Activation File (EAF) [5]. Note that, for W, we employ the self-shielding correction-factors obtained in [1] to the FISPACT calculations.

2.2.1. Fe and Cr

The gas production from Fe, as the primary constituent of steels, will be a major factor in determining the lifetime of near-plasma component in fusion reactors. Chromium (Cr), which forms around 10% of the composition of the reduced activation steels being proposed for fusion application, has a very similar transmutation profile to Fe [1], but has been included in the present study due to its prominence.

Figure 4 shows how the concentration of He and H produced under irradiation varies as a function

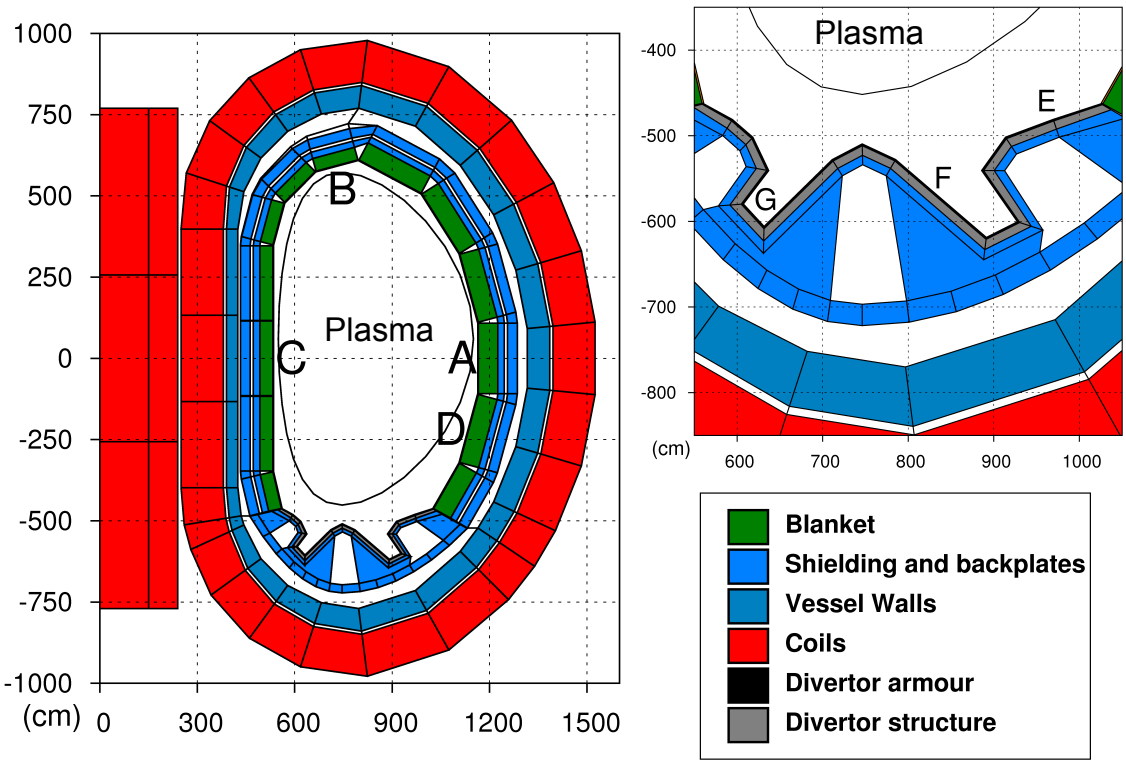

Figure 2: The simplified, homogeneous, DEMO model used in MCNP simulations to obtain neutron fluxes and spectra.

of time and of position on the FW of the DEMO model. The irradiation times shown here and elsewhere in this work are DEMO full-power years. In Cr, the gas concentrations are 20-25% lower than in Fe, but the variations as a function of time and position are similar.

At position B, the significant drop in gas production from Fe (and Cr) results from a combination of reduced total flux ($\sim 7 \times 10^{14}$ n cm^{-2} s^{-1} vs. $\sim 8 \times 10^{14}$ n cm^{-2} s^{-1} at the other positions) and a lower proportion of neutrons above the threshold energies for the gas producing reactions (e.g. (n, α)).

As a function of depth into the vessel, inventory calculations reveal that the changes in the neutron irradiation conditions (figure 3) cause the He (and H) production levels to fall significantly in Fe. For example, after 3 years under DEMO full-power conditions, the He concentration is around 400 atomic parts per million (appm) in the FW, but has barely reached 1 appm in the 20 cm backplate behind the blanket (see figure 5).

Note that the neutron spectra calculated by MCNP do not take into account time-dependent compositional changes in materials, such as those that will take place in the blanket as the Li is depleted during tritium breeding. It is possible to investigate these processes by using an inventory code, such as FISPACT, to periodically update the material compositions in an MCNP calculation. Packer *et al.* [6] have recently applied such a methodology to investigate how the tritium-breeding inventory evolves in the DEMO blanket.

2.2.2. W

While W (tungsten) will be present throughout a typical reactor vessel as small concentrations in most steels, it will be used in an almost pure form primarily in the high heat-flux divertor regions due to its high melting-point, thermal-conductivity, and resistance to sputtering and erosion [7]. In many reactor designs W is also considered for the FW armour layer [8].

For the present DEMO model the FW layer is very thin, meaning that it is almost transparent to neutrons, and so it is realistic to assume that the irradiation conditions found for FW on DEMO in the previous section are very close to those that would be obtained if the FW were W instead. The

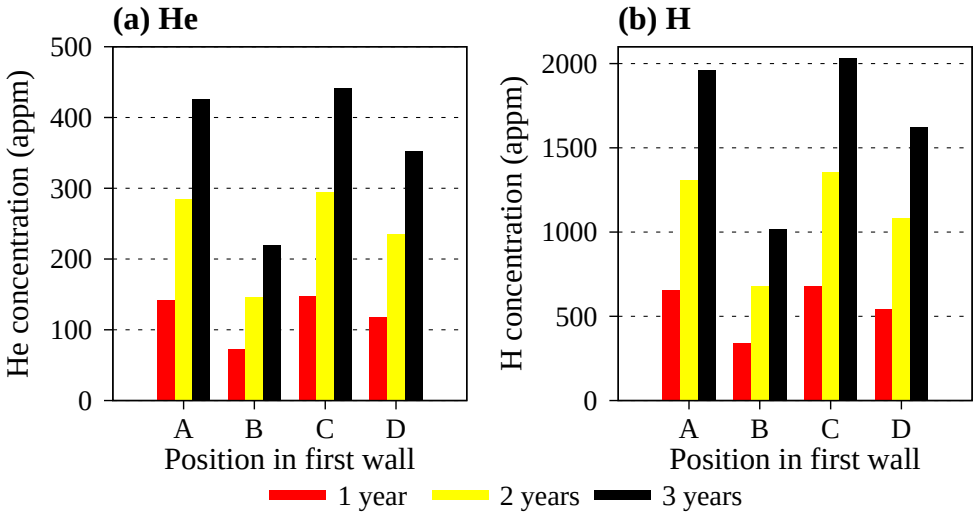

Figure 4: Variation in the (a) He, and (b) H, concentrations in pure Fe as a function of time for the spectra at different FW positions in DEMO – see figure 2.

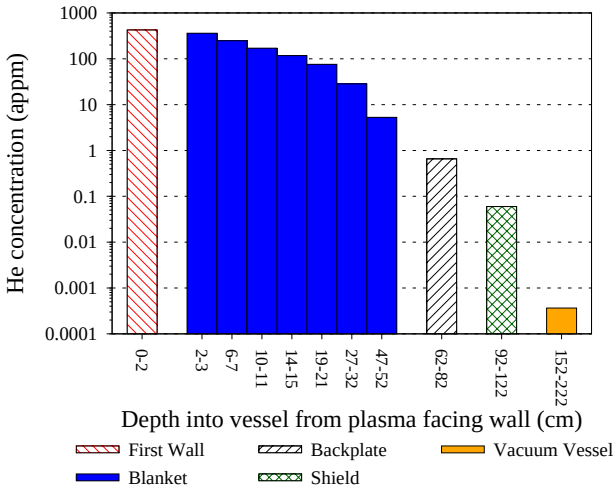

Figure 5: Variation in He concentration in pure Fe after a 3-year irradiation as a function of depth into the DEMO vessel at (A) in figure 2. Note the logarithmic scale of the concentration axes.

results from inventory calculations (figure 6) reveal that the concentration of He (and H) produced from pure W is very low, but can also vary significantly, even within the same layer of the divertor.

The amount of He produced in the divertor armour (see figure 2) after the first 3-years of irradiation varies from 9 appm at position E, to less than 1 (one) appm at G – an order of magnitude difference (figure 6a). In the divertor structure behind the armour the variation is similar, albeit at a systematically lower level. For H, the variations with position are similar but the absolute concentrations are roughly twice those found for He. The higher flux in the FW causes the gas concentration to be somewhat greater than those observed for the divertor (see figure 6).

Perhaps of greater significance for W, are the variations in Re concentration between the FW and the divertor (figure 6b), because of the potential for σ-phase precipitates (with Os) [9]. After 3 years in the FW at A, Re reaches a concentration of around 20000 appm (2 atomic %), which is broadly in line with the previous findings in [1]. However, in the divertor armour at position E, Re only reaches a concentration of around 6400 appm (1 at.%) on the same timescale.

2.2.3. Be

Beryllium, as the primary constituent of the blanket in the present DEMO model, has been found previously [1] to produce significant concentrations of He under neutron irradiation. For the present model, the inventory calculations indicate He concentrations in Be after 3-year irradiations of between 12000 appm in the first 1 cm of the equatorial blanket at position A in figure 2, to only 1200 appm in the final 5 cm (see figure 7). By comparison, H production in Be is around two orders of magnitude

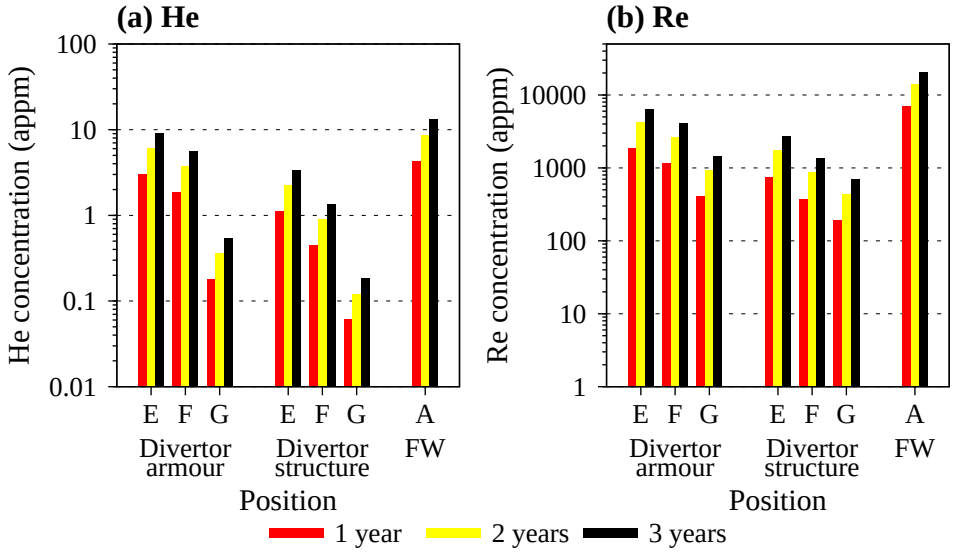

Figure 6: Variation in concentrations of (a) He, and (b) Re, produced in pure W under neutron irradiation as a function of position (and depth) in the divertor region of the DEMO design (figure 2).

less than for He, with, for example, only 230 appm produced in 3 years under the conditions calculated for the first centimetre of the DEMO blanket at A.

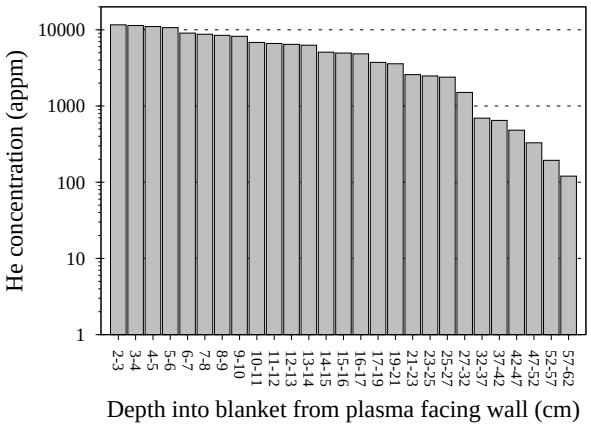

Figure 7: Variation in He concentration in pure Be after a 3-year irradiation as a function of depth into the DEMO blanket at (A) in figure 2.

3. Modelling of He accumulation at grain boundaries

The calculations described in the foregoing section produce quantitative estimates of the He production rates under any neutron-irradiation conditions. Using a simple model for He segregation to boundaries, we can use these results to estimate the timescales required to produce a sufficient amount of He to embrittle materials.

For a spherical grain:

$$N_{\mathrm{He}} \approx \frac{4}{3}\pi R^3 n G_{\mathrm{He}}, \tag{1}$$

where N_{He} is the total number of He atoms, G_{He} is the atomic concentration of He atoms in atomic parts per million (appm), and n is the atomic density of the material (cm^{-3}). If every He atom produced in a given grain migrates to the boundary, then

$$4\pi R^2 \nu_{\mathrm{He}} = \frac{4}{3}\pi R^3 n G_{\mathrm{He}},$$

where $\nu_{\mathrm{He}}$is the surface density of He, and so

$$\nu_{\mathrm{He}} = \frac{R}{3} n G_{\mathrm{He}}. \tag{2}$$

In a real grain there are likely to be internal obstacles that trap some of the He, but we neglect these here for simplicity.

Let us suppose that the grain boundaries begin to fail if the stored energy associated with the accumulated He is greater than (or equal to) the energy required to turn the boundaries into free surfaces. For the surface energy $\varepsilon_{\mathrm{surf}}$, which in the present work we estimate for different materials using experimental values from [10], and the energy of so-

lution for a He atom E_{He}^{sol} we thus have:

$$E_{\mathrm{He}}^{\mathrm{sol}}\nu_{\mathrm{He}}^{c} \approx 2\varepsilon_{\mathrm{surf}}, \quad (3)$$

where ν_{He}^{c} is the critical density required to bring-about boundary destabilization. Once ν_{He}^{c} is known, the critical bulk He concentration G_{He}^{c} can be obtained from equation (2).

Using average values for E_{He}^{sol} (*i.e.* averaged over different positions) [11, 12, 13, 14], we find the G_{He}^{c} values for a grain size of 0.5 μm in different materials given in table 1, with other elemental quantities taken from [15]. Unsurprisingly, Be, having a low atomic density n, has the lowest G_{He}^{c} value and so it is likely to be more susceptible than most to He-induced grain-boundary embrittlement.

Table 1 also shows estimates of the critical lifetimes t_{He}^{c} associated with the G_{He}^{c} values for each material. In this case we have performed FISPACT calculations using the FW irradiation conditions predicted for the FW of DEMO at A in figure 2.

Be has the lowest estimated lifetime; only 22 days. Meanwhile Ta and W, have high critical densities and very slow He production rates, producing large lifetimes; more than 200 years for these small 0.5 μm grains.

As an illustration of how critical the material grain size R is in these calculations consider the effect of increasing the grain size in Fe by an order of magnitude. Under such circumstances, $t_{\mathrm{He}}^{c} \approx$ 4 years for the 0.5 μm grain radius (table 1), but is only 4 months if the effective size of grains is 5 μm.

4. Summary

The MCNP calculations on the conceptual design of the DEMO fusion reactor show that the neutron irradiation conditions can vary significantly as a function of position within the reactor. Even in the same component the flux can change dramatically over short distances. As a function of depth into the first wall the flux drops by several orders of magnitude and the energy spectrum becoming considerably softer.

The FISPACT-inventory calculations reveal how the variation in conditions influence the transmutation of materials. In Fe (and therefore in steels) for example, the gas concentrations fall by many order of magnitude from the thin FW layer to the outer regions of the vessel, such as the shield. While the production of He is likely to be significant for the FW (concentrations in the range of 400 appm are known to cause a change fracture behaviour of neutrons-irradiated steels compared to those exposed to neutrons alone [16]), it will quickly become unimportant in regions further from the plasma.

In W the predicted gas concentrations are probably too low to have any impact on component lifetime. However, further work is needed to quantify the acceptable levels of other impurities in W, such as Re, Ta, and Os, because these can reach non-negligible levels.

In Be, the inventory calculations confirm the previous findings [1], and show that He can be produced in large amounts in the inner regions of the blanket. However, the production rate tails off rapidly as the conditions change through the blanket, so that by its outer edge the He concentrations are roughly two orders of magnitude smaller than at the inner, near-plasma edge. This large variation is likely to produce non-homogeneous changes to structural and mechanical properties across the full depth of the blanket, especially since Be is known to swell significantly under neutron irradiation [17, 18].

Even worse for Be, are the results from the modelling of grain-boundary embrittlement. The estimates suggest that Be would suffer very significantly from embrittlement after relatively short periods of time in a fusion reactor. In other materials, the situation is less bad, with the prospect, for example, of Fe being perfectly adequate for structural purposes on commercially viable timescales.

Acknowledgments

This work was funded by the RCUK Energy Programme under grant EP/I501045 and the European Communities under the contract of Association between EURATOM and CCFE. The views and opinions expressed herein do not necessarily reflect those of the European Commission. This work was carried out within the framework of the European Fusion Development Agreement.

References

[1] Gilbert M R and Sublet J -Ch, 2011, *Nucl. Fus.*, **51** 043005

[2] Zheng S Preliminary Evaluation of Decay Heat in Fusion HCPB DEMO Reactor; presented at the 4th IAEA-TM on First Generation Fusion Power Plants - Design and Technology, 8-9 June 2011, Vienna

Table 1: Table of calculated critical boundary densities ν^c_{He}, critical bulk concentrations G^c_{He}, and approximate critical lifetimes t^c_{He} (in DEMO first-wall full-power time) for He in various elements.

Element	ν^c_{He} (cm^{-2})	R (μm)	G^c_{He} (appm)	t^c_{He}-DEMO (FW time)
Fe	6.76×10^{14}	0.5	478.1	4 years
V	8.59×10^{14}	0.5	713.2	15 years
Cr	5.53×10^{14}	0.5	398.6	4 years
Mo	7.31×10^{14}	0.5	684.1	16 years
Nb	8.96×10^{14}	0.5	968.2	21 years
Ta	9.25×10^{14}	0.5	1001.2	283 years
W	7.51×10^{14}	0.5	714.3	244 years
Be	4.80×10^{14}	0.5	233.0	22 days
Zr	8.82×10^{14}	0.5	1231.7	40 years

[3] Brown F B, Barrett R, Booth T, Bull J, Cox L, Forster R, Goorley J, Mosteller R, Post S, Prael R, Selcow E, Sood A, and Sweezy J, 2002, *Trans. Am. Nucl. Soc.*, **87** 273

[4] Forrest R A, FISPACT-2007: User manual, UKAEA FUS 534, 2007

[5] Forrest R A, The European Activation File: EAF-2003 overview, UKAEA FUS 484, 2002

[6] Packer L W, Pampin R, and Zheng S, 2011, *J. Nucl. Mater.* in press

[7] Nemoto Y, Hasegawa A, Satou M, and Abe K, 2000, *J. Nucl. Mater.*, **283–287** 1144–1147

[8] Maisonnier D, Cook I, Sardain P, Boccaccini L, Bogusch E, De Pace L, Forrest R, Giancarli L, Hermsmeyer S, Nardi C, Norajitra P, Pizzuto A, Taylor N, and Ward D, 2005, *Fusion Eng. Des.*, **75–79** 1173–1179

[9] Cottrell G A, 2004, *J. Nucl. Mater.*, **334** 166–168

[10] Vitos L, Ruban A, Skriver H, and Kollár J, 1998, *Surf. Sci.*, **411** 186–202

[11] Willaime F and Fu C C, 2006, *Mater. Res. Soc. Symp.*, **981** 0981–JJ05–04

[12] Middleburgh S C and Grimes R W, 2011, *Acta Mater.* in press

[13] Ganchenkova M G, Vladimirov P V, and Borodin V A, 2009, *J. Nucl. Mater.*, **386–388** 79–81

[14] Koroteev Yu M, Lopatina O V, and Chernov I P, 2009, *Phys. Solid State*, **51** 1600–1607

[15] Lide D R, editor, 2004, *CRC Handbook of Chemistry and Physics* (CRC Press, Boca Raton, Florida) 85th edition

[16] Yamamoto T, Odette G R, Kishimoto H, Rensman J W, and Miao P, 2006, *J. Nucl. Mater.*, **356** 27–49

[17] Chakin V P, Posevin A O, and Kupriyanov I B, 2007, *J. Nucl. Mater.*, **367–370** 1377–1381

[18] Möslang A, Pieritz R A, Boller E, and Ferrero C, 2009, *J. Nucl. Mater.*, **386–388** 1052–1055